Journal of Natural Sciences Research www.iiste.org
ISSN 2224-3186 (Paper) ISSN 2225-0921 (Online)
Vol.3, No.10, 2013

Mineralogy and Geochemical Appraisal of Paleo-Redox Indicators in Maastrichtian Outcrop Shales of Mamu Formation, Anambra Basin, Nigeria

Akinyemi[1], S. A., Adebayo[1], O. F., Ojo[1], O. A., Fadipe[2], O. A., Gitari[3], W. M.
1. Department of Geology, Faculty of Science, Ekiti State University Ado Ekiti, Private Mail Bag 5363, Ado Ekiti, Nigeria.
2. Petroleum Analytical Laboratory, Department of Earth Sciences; University of the Western Cape, Private Bag X17, Bellville 7535, South Africa.
3. Environmental Remediation and Water Pollution Chemistry Group, Department of Ecology and Resources Management, School of Environmental Studies, University of Venda. Private Bag, X5050, Thohoyandou, 0950, South Africa.
* E-mail of the corresponding author: akinyemi70@gmail.com

Abstract
The Mamu Formation exhibits two types of shales, viz. grey and dark shales. The geochemical and mineralogical compositions of these shales were investigated using X-ray fluorescence (XRF) and Laser Ablation- Inductively Coupled Plasma Spectrometry (LA-ICPMS) and X-ray diffraction techniques. The basal part of the section is characterized by presence of quartz and kaolinite as the major crystalline minerals with minor quantity of hematite. The presence of hematite in the basal part of the shale sequence suggests oxidizing diagenetic environment of deposition. The second geochemically specific interval (upper part) is characterised by quartz and kaolinite as major crystalline minerals with traces of halloysite and grossite. The ternary plot of these major elements indicates the majority of shale samples examined are variably enriched with SiO_2 relative to Al_2O_3 and CaO. The positive correlations of K_2O, TiO_2, and Na_2O, with Al_2O_3 indicate that these elements are associated entirely with detrital phases. Some trace elements such as Cr, Ni, and V are positively correlated with Al_2O_3 which suggest that these elements may be bound in clay minerals and concentrated during weathering. The K_2O/Al_2O_3 ratio is close to the lower limit of clay mineral range, which suggests that kaolinite is the dominant clay minerals. The Al_2O_3/TiO_2 and low Cr/Ni ratios suggest that felsic components were the main components among the basement complex source rocks. The geochemical indices such as Th/Cr, Cr/Th, Th/Co and Th/Cr ratios suggest that these shales were derived from felsic source rocks. The chemical index of alteration values indicates that these shales have experienced strong chemical weathering at the source area. In addition, the depletion of Na and Ca also illustrates an intense chemical weathering of the source rocks. The mineralogical index of alteration values of the studied shale samples indicates an intense to extreme weathering of mineralogical components. The shale units exhibits different degrees of trace-element enrichment, with the approximate order of enrichment relative to an average shale being Co > Pb > Ni > Zr > Cu > Rb > V > Cr > Ba > V > Sr > U. The inverse correlation between Eh, pH, EC and TDS in outcrop Maastrichtian shale samples suggests well oxygenated environment of deposition. In addition, based on previously established thresholds, V/Cr, Ni/Co, Cu/Zn and U/Th ratios support that these shales were deposited under oxidizing diagenetic environment.
Keywords: mineralogy, geochemistry, paleo-redox conditions, trace element enrichments, shales, Mamu Formation, Anambra basin, Nigeria.

1. Introduction

Trace elements commonly exhibit considerable enrichment in laminated, organic- rich facies, especially those deposited under euxinic conditions and, conversely, little if any enrichment in bioturbated, organic-poor facies (Wedepohl, 1971; Calvert and Pedersen, 1993; Algeo and Maynard, 2004). The geochemical behaviour of trace elements in modern organic rich fine grained sedimentary rocks (i.e. shales) and anoxic basins has often been discussed (Brumsack, 1989; Calvert and Pedersen, 1993; Warning and Brumsack, 2000; Algeo and Maynard, 2004). Redox-sensitive trace element (TE) concentrations or ratios are among the most widely used indicators of redox conditions in modern and ancient sedimentary deposits (e.g., Calvert and Pedersen, 1993; Jones and Manning, 1994; Crusius et al., 1996; Dean et al., 1997, 1999; Yarincik et al., 2000; Morford et al., 2001; Pailler et al., 2002; Algeo and Maynard, 2004). Enrichments of redox-sensitive elements reflect the depositional environment of ancient organic carbon-rich sediments and sedimentary rocks as well and can, therefore, be used to elucidate the likely palaeoceanographic conditions leading to their formation (Brumsack, 1980, 1986; Hatch and Leventhal, 1992; Piper, 1994).
Anambra Basin, the first area where intensive oil exploration was carried out in Nigeria, has about 12,000 metre

of sedimentary rocks which accumulated in its thickest part since the Cretaceous time (Agagu and Adighije, 1983). The dominant lithologies comprise sandstones, shales, limestones and coal seams. The unrewarding initial oil exploratory effort in the basin led to its neglect by most researchers in favour of the nearby Niger Delta Basin which has been prolific in terms of oil and gas exploration and production. With less than 50 wells so far drilled (two discoveries; Anambra River-1, Ihadagu-1) and very scanty 2-D seismic information, Anambra Basin is under explored. Again, a simple statistical analysis of the literature review shows that more than ninety percent of the studies so far in the basin are in the southeast section (Unomah and Ekweozor, 1993; Akaegbobi and Schmitt, 1998; Adebayo and Ojo, 2004; Ojo *et al.*, 2009; Chiaghanam *et al*., 2012).

Since the search for crude oil in commercial quantity in the basin still remained a source of concern for oil companies and research groups, a better understanding of the paleo-redox and paleogeographic conditions of the outcrops will benefit the oil companies that had secured concession blocks in the basin; and those that may wish to use this information for deep-water exploration in the Niger Delta Basin. This is because some of these outcrops packages are said to be equivalent to the lithostratigraphic units within the subsurface of the Niger Delta (Short and Stauble, 1967).

In this study, we present the inorganic geochemical data for Maastrichtian shale outcropped at Auchi-Igarra road, Anambra Basin, Nigeria. This is to determine the provenance, redox conditions of depositional environment, and element enrichments of the studied Maastrichtian shale sequence. The purpose of this paper is in two folds; (1) to contribute and discuss a wide range of trace metal to the geochemical data set of the Maastrichtian shale outcrop which are lacking in the current literature (2) to assess the use of well known geochemical proxies (i.e. Ni/Co, V/Cr, Cu/Zn and U/Th) for discerning paleogeographical conditions of the shale sequence.

2. Geological setting of Anambra basin

Anambra Basin is located in the southeastern part of Nigeria. It is bordered in the south by the Niger Delta Complex, to the west by the West African massif, to north by Bida Basin and Northern Nigerian massif, and delimited in the east the Middle Benue Trough and Abakaliki Anticlinorium (Figure 1). The basin lies between longitudes 6.3^0E and 8.0^0E, and latitudes 5.0^0N and 8.0^0N. Anambra Basin in Nigeria is considered by some authors as the Lower Benue Trough, a NE-SW trending, folded, aborted rift basin that runs obliquely across Nigeria (Figure 1). Hence its origin was linked to the tectonic processes that accompanied the separation of the African and South American plates in the Early Cretaceous (Murat, 1972; Burke *et al.*, 1996). The rift model had been supported by evidence garnered by structural, geomorphic, stratigraphic and paleontologic studies (Reyment, 1969; Burke *et al.*, 1972; Benkhelil, 1989; Guiraud and Bellion, 1995). The evolution of the basin represents the third cycle in the evolution of the trough and its associated basins when the Abakaliki Trough was uplifted to form the Abakaliki Anticlinorium whilst the Anambra Platform was downwarped to form the Anambra Basin (Murat, 1972; Weber and Daukoru, 1975) resulting in the westward displacement of the trough's depositional axis. Its sedimentation trend is patterned by the shifting of depocentres.

A great deal of work had been done to elucidate the age, paleoenvironment, paleogeography, sedimentary tectonics, origin of the deposits, the litho- and biostratigrapy and hydrocarbon (or fossil fuel) potentials of the basin (Reyment, 1965; Murat, 1972; Salami, 1983; Agagu *et al*., 1985; Allix, 1987; Akande *et al*., 1992; Nwajide and Reijers, 1996, Akande, 2007). The sequence of depositional events suggests a progressive deepening of the basin from lower coastal plain and shoreline deltas to shoreline and shallow marine deposits (Arua, 1986; Anyanwu and Arua, 1990; Fayose and Ola, 1990). The resulting succession comprises the Nkporo Group, Mamu Formation, Ajali Sandstone, Nsukka Formation, Imo Formation and Ameki Group (Table 1). The detailed stratigraphic description of these formations is available in several publications (Petters, 1978; Agagu et al. 1985; Reijers, 1996). The rich coal deposits of Late Campanian – Early Maastrichtian ages suggest brackish environment during their deposition.

3. Methodology/research approach

3. Materials and method

3.1 Sampling technique

Exposed Maastrichtian shale outcrop located at Auchi-Igarra road, Edo state, Nigeria (07º 05.071'N, 006º14.826E; 162.72m above sea level) (Fig. 2) was sampled. 500 grams of shale samples were collected at an interval of 0.2m from the shale sequence. All the 10 shale samples were immediately stored in zip lock polyethylene bag and preserved at room temperature. The samples were dried at 60ºC, crushed to fine powder and homogenized in an agate ball mill. The pulverized shale samples were analysed with XRD, XRF and LA-ICPMS techniques.

3.2. XRF and LA-ICPMS analyses

The elemental data for this work have been acquired using X- ray fluorescence (XRF) and Laser Ablation-inductively coupled plasma spectrometry (LA-ICPMS) analyses.

The analytical procedures are as follows;
Pulverised shale samples were analysed for major element using Axios instrument (PANalytical) with a 2.4 kWatt Rh X-ray Tube. Further, the same set of samples were analysed for trace element using LA-ICPMS instrumental analysis. LA-ICP-MS is a powerful and sensitive analytical technique for multi-elemental analysis. The laser was used to vaporize the surface of the solid sample, while the vapour, and any particles, were then transported by the carrier gas flow to the ICP-MS. The detailed procedures for sample preparation for both analytical techniques are reported below.

3.2.1. Fusion bead method for Major element analysis

- Weigh 1.0000 g ± 0.0009 g of milled sample
- Place in oven at 110 ºC for 1 hour to determine H_2O^+
- Place in oven at 1000 ºC for 1 hour to determine LOI
- Add 10.0000 g ± 0.0009 g Claisse flux and fuse in M4 Claisse fluxer for 23 minutes.
- 0.2 g of $NaCO_3$ was added to the mix and the sample+flux+$NaCO_3$ was pre-oxidized at 700 °C before fusion.
- Flux type: Ultrapure Fused Anhydrous Li-Tetraborate-Li-Metaborate flux (66.67 % $Li_2B_4O_7$ + 32.83 % $LiBO_2$) and a releasing agent Li-Iodide (0.5 % LiI).

3.2.2. Pressed pellet method for Trace element analysis

- Weigh 8 g ± 0.05 g of milled powder
- Mix thoroughly with 3 drops of Mowiol wax binder
- Press pellet with pill press to 15 ton pressure
- Dry in oven at 100 ºC for half an hour before analysing.

These analytical methods yielded data for eleven major elements, reported as oxide percent by weight [SiO_2, TiO_2, Al_2O_3, Fe_2O_3, MgO, MnO, CaO, Na_2O, K_2O, Cr_2O_3 and P_2O_5] and 21 trace elements [Ni, Cu, Zn, Ga, Rb, Sr, Y, Zr, Nb, Co, V, Pb, Th, U, Ti, Cr, Ba, La, Ce, Nd and P] reported as mg/kg (ppm).

3.3. Loss on ignition determination

Loss on Ignition (LOI) is a test used in XRF major element analysis which consists of strongly heating a sample of the material at a specified temperature, allowing volatile substances to escape or oxygen is added, until its mass ceases to change. The LOI is made of contributions from the volatile compounds of H_2O^+, OH^-, CO_2, F^-, Cl^-, S; in parts also K^+ and Na^+ (if heated for too long); or alternatively added compounds O_2 (oxidation, e.g. FeO to Fe_2O_3), later CO_2 (CaO to $CaCO_3$). In pyro-processing and the mineral industries such as lime, calcined bauxite, refractories or cement manufacturing industry, the loss on ignition of the raw material is roughly equivalent to the loss in mass that it will undergo in a kiln, furnace or smelter.

3.4 Mineralogical analysis

Pulverised shale samples were analysed for mineralogical composition by X-ray diffraction (XRD) analysis. A Philips PANalytical instrument with a pw 3830 X-ray generator operated at 40 kV and 25 mA was used. The pulverised samples were oven dried at 100 °C for 12 h to remove the adsorbed water. The samples were pressed into rectangular aluminium sample holders using an alcohol wiped spatula and then clipped into the instrument sample holder. The samples were step-scanned from 5 to 85 degrees on 2 theta scale at intervals of 0.02 and counted for 0.5 sec per step.

3.5 pH of the interstitial pore water of the shales

The pH of interstitial/pore water was determined using 1:10 shale: water ratio. Ten grams of each of the shale samples were weighed and put in a beaker and suspended in 100 ml of ultra pure water. The mixture was then agitated thoroughly for 30 min, and allowed to settle for 15 min. The pH, EC, TDS and Eh of the supernatant were recorded. The filterate was analyzed for anions using ion chromatography and cations using inductive coupled plasma optical emission spectroscopy (ICP-OES). Triplicate analysis was carried out in each case.

3.6 Data treatment and multivariate statistical methods

Multivariate statistical method was applied on the bulk chemical data obtained from the XRF analysis of the studied shale samples using SPSS-17.0 statistical software. Varimax rotated factor analysis was performed on correlation matrix of the reorganized data of the samples. The variance, cumulative, and extraction sums of square loadings of the variables with Eigen-values were computed. Rotation of the axis defined by factor analysis produced a new set of factors, each one involving primarily a sub-set of the original variables with a little overlap as possible, so that the original variables were divided into groups.

The factor analysis of these data set was further sorted by the contribution of the less significant variables (< 0.4 factor score). A varimax rotation (raw) of the different varifactors of eigen-value greater than 1, were further cleaned up by this technique and in varifactors original variables participated more clearly. Liu *et al*. (2003a) classified the factor loading as “strong”, “moderate”, and “weak”, corresponding to absolute loading values of > 0.75, 0.75–0.50, and 0.50–0.40, respectively. Factor and cluster analyses were combined to assess the degree of major component matrix dissolution and determination of chemical processes. Hierarchical agglomerative

clustering was performed on data normalized to z scores and unit variance using squared Euclidean distances as the measure of similarity (Massart *et al*., 1988). Wards method was selected because it possesses a small space distorting effect, uses more information on cluster contents than other methods (Helena *et al*., 1999), and has been proven to be an extremely powerful grouping mechanism (Willet, 1987). This multivariate statistical approach enables the description of the best discriminatory parameters of the studied shale units on the basis of a simultaneous approach of geochemical and mineralogical data.

4. Results and discussion

4.1. Lithological description

In the outcrop section, on the Auchi-Igarra road (Figure 2 & 3) the argillaceous units are not well exposed. The approximately 1.6m thick sequence exposed along Auchi-Igarra road (Figure 2 & 3) consists predominantly of shales and mudstones. At the basal part of the section is prominent shale bed with an average thickness of 0.2m, it is dark greyish with brownish specs, fine grained in texture, highly fissile with tracks. The shale unit within depth interval of 0.4-1.0m is dark greyish coloured with brownish specs, fine grained in texture which are rhythmically interbedded with concretional to massive, bioturbated mudstones. The upper part of the outcrop section (1.2-1.6m) is light greyish, brownish with reddish brown specs. The shales are fine grained, mixed with clay and mudstones and contains abundant woody fragments and plant remains. The argillaceous sediments (shales and mudstones) in this section are interpreted to have been deposited in a low-energy setting, probably in a restricted body of water (Braide, 1992). The abundance of land derived woody and plant materials suggest freshwater conditions (Obaje et al., 2011). The fine-grained argillaceous sediments and sandstones in the upper part of the section are interpreted as shelf or flood plain deposits (Garrels and Makenzie, 1971).

4.2. Mineralogical composition

The mineral composition of the shale samples are predominantly characterized by quartz and kaolinite, which were found in all samples. X-Ray diffraction analyses show little mineralogical variation between shale samples within geochemically specific intervals. The first interval is from 0.0 to 0.2m depth. It is characterized by the presence of quartz and kaolinite as the major crystalline minerals with minor quantities of hematite (Figure 4a). The second geochemically specific interval is at the depth of 0.6 - 2m, and is characterised by quartz and kaolinite as major crystalline minerals with minor quantities of halloysite and grossite (Figure 4b). Kaolinites are indicators for its detrital origin in continental sediments (Kassim, 2006). Furthermore, Weaver (1960) stated that kaolinite is dominant in sediments of fluviatile environments.

Kaolinite is known to be concentrated in many near-shore sediments and to decrease in abundance with distance from the shoreline as other clay minerals increase (Parham, 1966). Robert and Kennett (1994) reported that increased kaolinite contents in marine sediments resulted either from increased runoff, which could be caused by sea level falls, or from increased rainfall. Kaolinite is formed under a good drainage system where the water travel distance was much greater, less rapid flushing of sediments and less removal of silica (Berner and Berner, 1996). Halloysite, which consists of a poorly ordered arrangement of kaolinite-like units, with variable amounts of water between the layers, generally between 0.6 to 4H2O per formula unit, and often with a tabular form.

Hematite is the oxidation products of weathered ferrous minerals and constitutes a major source of detrital iron in sediments. During diagenesis limonite may be dehydrated to hematite. In order for this to happen, the original sediment would have to be relatively free from decomposable organic matter so a high enough oxidation/reduction potential (Eh) can be maintained to stabilize hematite. As a result, organic matter is generally abundant in marine sediments; almost all hematite are non marine (Berner, 1971). Consequently, the presence of hematite in the bottom layers of the shale sequence suggest non marine environment of deposition.

4.3. pH, EC and Eh of interstitial pore water

The mean pH measured in the Maastrichtian shales was 6.3, and range of variation was 5.9 - 8.1 (Table 2). A simple correlation analysis revealed that the pH values were very closely correlated with electrical conductivities (EC), total dissolved solids (TDS), Ca, Mg, Na, K and F. The inverse correlation between Eh and pH, EC and TDS in the samples suggests well oxygenated environment of deposition. Similarly, Eh showed inverse correlation with Ca, Mg, Na, K and F (Table 2).

4.4. Major and trace elements characteristics and provenance

Marine shales and mud rocks can be regarded as an admixture of three end-member oxides: SiO_2 (detrital quartz and/or biogenic silica), Al_2O_3 (clay fraction) and CaO (carbonate content) (Ross and Bustin, 2009). The ternary plot of the major elements indicate that majority of the shale samples examined are enriched with SiO_2 relative to Al_2O_3 and CaO (Fig. 5).

The studied shale samples show high content of SiO_2 with small variations (~51.83 – 92.00) (Table 3). The Al_2O_3 content shows low concentrations with large variations (~3.42 – 26.46). Aluminium concentration is a reasonably good measure of detrital flux (Nagarajan, 2007), the positive correlations of K_2O, TiO_2, and Na_2O, with Al_2O_3 (linear correlation coefficient r = 0.98, 0.79, and 0.14, respectively, number of samples (n) = 10)

indicate that these elements are associated entirely with detrital phases. Some trace elements such as Cr, Ni, and V are positively correlated with Al_2O_3 (r = 0.155, r = 0.009, and r = 0.043 respectively) which suggest that these elements may be bound in clay minerals and concentrated during weathering (Fedo *et al*., 1996; Nagarajan *et al*., 2007).

The SiO_2/Al_2O_3 ratio of the studied shale samples is shown in the Table 3. Felix (1977) established that the SiO_2/Al_2O_3 ratio for pure montmorillonite ranges from 2.80 to 3.31 while for pure kaolinite it is about 1.18. The SiO_2/Al_2O_3 ratio for these shale samples varies between (1.96 and 26.95) which are higher than that of pure kaolinite and montmorillonite. Perhaps, this indicates that the clay mineralogy of the studied shale samples consists mainly kaolinite and/or a mixture of kaolinite and halloysite. This is confirmed by mineralogical analysis results (Figure 4b).

The K_2O/Al_2O_3 ratio of sediments can be used as an indicator of the original composition of ancient sediments. The K_2O/Al_2O_3 ratios for clay minerals and feldspars are different (0.0 to 0.3, 0.3 to 0.9, respectively; Cox *et al.,* 1995). The K_2O/Al_2O_3 ratios vary from 0.04 – 0.05 in the studied shale samples (Table 3). In most of the shale samples, the K_2O/Al_2O_3 ratios are close to the lower limit of clay mineral range, which suggests that kaolinite is the dominant clay minerals in these samples as revealed by XRD spectra analysis (Figure 4). The abundance of Si, Al, Ti and K in shales may be perturbed from parent material by weathering, transport and depositional processes (Nesbitt *et al*. 1980). According to Gill and Yemane (1996) the Na_2O/K_2O ratios indicate salinization by intense weathering or extreme leaching. The studied shale samples show low Na_2O/K_2O ratios (Table 3), which indicate no evidence of salinization.

The geochemical signatures of clastic sediments have been used to find out the provenance characteristics (Condie *et al.,* 1992; Cullers, 1995; Madhavaraju and Ramasamy, 2002; Armstrong-Altrin *et al*., 2004; Nagarajan, 2007). Al_2O_3/TiO_2 ratios of most clastic rocks are essentially used to infer the source rock compositions, because the Al_2O_3/TiO_2 ratio increases from 3 to 8 for mafic igneous rocks, from 8 to 21 for intermediate rocks, and from 21 to 70 for felsic igneous rocks (Hayashi *et al.,* 1997). In the studied shale samples, the Al_2O_3/TiO_2 ratio ranges from 11.96 - 24.06 (Table 3).

Accordingly, the Al_2O_3/TiO_2 ratios suggest that intermediate to felsic granitoid rocks must be the probable source rocks for the shale samples in the present study. The abundance of Cr and Ni in siliciclastic sediments are considered as a useful indicator in provenance studies. According to Wrafter and Graham (1989) a low concentration of Cr indicates a felsic provenance, and high contents of Cr and Ni are mainly found in sediments derived from ultramafic rocks (Armstrong-Altrin *et al.,* 2004). Chromium and nickel concentrations are low in the studied shale samples (Table 3). Consequently, the low Cr/Ni ratios (i.e. 3.76 – 27) indicate that felsic components were the main components among the basement complex source rocks. Ratios such as La/Sc, Th/Sc, Th/Co, and Th/Cr are significantly different in felsic and basic rocks and may allow constraints on the average provenance composition (Wronkiewicz and Condie, 1990; Cox *et al*., 1995; Cullers, 1995). The ratios of Th/Cr (~0.036 – 0.09), Cr/Th (~8.1 – 14.15), Th/Co (~0.006 – 0.68) and Th/Cr (~0.036 – 0.09) suggests that the shale samples in the present study were derived from felsic source rocks (Cullers, 1994; 2000; Nagarajan, 2007).

The chemical index of alteration (CIA) defined as CIA = 100 x $Al_2O_3/ (Al_2O_3 + CaO + Na_2O + K_2O)$ have been established as a general indicator of the degree of weathering in any source regions (Nesbitt and Young, 1982; Fedo et al., 1995). In the equation, CaO* is the amount of CaO incorporated in the silicate fraction of the studied shale samples. Correction for CaO from carbonate contribution was not done for the studied shale samples since there was no CO_2 data. Thus, to compute for CaO* from the silicate fraction, the assumption proposed by Bock et al. (1998) was adopted. In this regard, CaO values were accepted only if $CaO \leq Na_2O$; consequently, when $CaO > Na_2O$, it was assumed that the concentration of CaO equals that of Na_2O (Bock et al., 1998). However, only one brownish coloured shale sample (C2.0m) showed CaO contents higher than Na_2O. High values (i.e.76-100) indicate intensive chemical weathering at the source area whereas low values (i.e., 50 or less) indicate unweathered source areas. The CIA values (Table 3) indicate that the studied shale samples have experienced strong chemical weathering (CIA > 90) at the source area. In addition, the depletion of Na and Ca illustrates an intense chemical weathering of the source rocks. As Al_2O_3, CaO, Na_2O and K_2O are related with CIA, they reveal variations between the investigated samples reflecting variable climatic zones or rates of tectonic uplift in source areas. The mineralogical index of alteration indicates the degree of weathering for each analysed sample, independent of the depth of sampling. The calculation of the mineralogical index of alteration (MIA), according to Voicu et al., (1997) is: MIA = 2*(CIA-50).

These ranges of MIA values indicate incipient (0-20%), weak (20-40%), moderate (40-60%), and intense to extreme (60-100%) weathering. The value of 100 % means complete weathering of a primary material into its equivalent weathered product (Voicu and Bardoux, 2002). The MIA value of the studied shale samples range from 83.49 – 90.03 (Table 2), therefore indicating an intense to extreme weathering of the mineralogical components of the source rock.

4.5. Paleo-redox conditions and trace element enrichments

Some trace element ratios such as Ni/Co, V/Cr, Cu/Zn and U/Th have been used to evaluate paleoredox conditions (Hallberg, 1976; Jones and Manning, 1994). The ratio of uranium to thorium may be used as a redox indicator with U/Th ratio being higher in organic rich mudstones (Jones and Manning, 1994). U/Th ratios below 1.25 suggest oxic conditions of deposition, whereas values above 1.25 indicate suboxic and anoxic conditions (Jones and Manning, 1994; Nath *et al*., 1997). The present study shows low U/Th ratio (~0.13), which indicate that these shale samples were deposited in an oxic environment. A few numbers of authors have used V/Cr ratio as an index of paleooxygenation (Dill, 1986; Dill *et al.,* 1988; Nagarajan, 2007). Bjorlykke (1974) reported the incorporation of Cr in the detrital fraction of sediments and its possible substitution for Al in the clay structure. Vanadium may be bound to organic matter by the incorporation of V^{4+} into porphyrins, and is generally found in sediments deposited in reducing environments (Shaw *et al.,* 1990). According to Jones and Manning (1994), the V/Cr ratios above 2 indicate anoxic conditions, whereas values below 2 suggest more oxidizing conditions. In the present study, the V/Cr ratios of all the shale samples vary between 1.01 and 1.91, which indicates that they were deposited in an oxic depositional environment.

Several authors have used the Ni/Co ratios as a redox indicator (Dypvik, 1984; Dill, 1986; Nagarajan, 2007) Jones and Manning (1994) showed that the Ni/Co ratios below 5 indicate oxic environments, whereas ratios above 5 suggest suboxic and anoxic environments. The Ni/Co ratios in this study vary between 0.11-1.04 (Table 2) suggesting that these shale samples were deposited in a well oxygenated environment. The Cu/Zn ratio is also used as a redox parameter (Hallberg, 1976). According to Hallberg (1976) high Cu/Zn ratios indicate reducing depositional conditions, while low Cu/Zn ratios suggest oxidizing conditions. Therefore, the low Cu/Zn ratios in the studied shale samples (Table 3) indicate that they were deposited under oxidizing conditions.

The enrichment factors (EF) were determined by normalizing each trace element to Al, which is understood to suggest the detrital influx, and comparing these ratios to those of normal shale. The enrichment factor (EF) is equal to (Element/Al) / (Element/Al) shale, where the ratio in the numerator is that for the shale in question, and the ratio in the denominator is that for a‘‘typical’’ shale (using data from Wedepohl, 1971). This approach has been used by several authors to evaluate trace-element enrichments in modern and ancient sediments (e.g., Calvert and Pedersen, 1993; Arnaboldi and Meyers, 2003; Rimmer, 2004). The trace elements data in the studied shale samples show different levels of enrichment (Table 4).

Based on enrichment factor (EF) values, the magnitude of enrichment differs, with Co (~0.06-41.82) and Pb (~0.61-30.05) peaked at the bottom in the shale sequence. The enrichment factor levels of Ni (~0.07-5.49) and Zr (~0.33-3.59) peaked at the thickness of 0.8m and bottom respectively. The enrichment factor levels of Cu (~0.11-2.05) and (~0.21-1.60) show maxima at 0.4m and 0.2m thickness respectively in the shale sequence. Enrichment factor values of V (~0.43-1.55) and Cr (~0.71-1.52) has the highest magnitude levels at the bottom in the shale sequence. The enrichment factor levels of Ba (~0.28-1.31) and Zn (~0.18-1.30) peaked at 0.60m thickness in the shale sequence. The enrichment factor levels of Sr (~0.22-1.19) and U (~0.00-0.46) show maxima at 0.6m and 0.2m thickness respectively in the shale sequence. The estimated order of enrichment relative to typical shale is Co > Pb > Ni > Zr > Cu > Rb > V > Cr > Ba > V > Sr > U (Table 4).

4.6. Factor analysis of the geochemical data

The varimax rotated factor loadings matrix and communalities were obtained from principal component analysis (PCA). PCA is a statistical tool used to assess metal behaviour in earth materials (Liu et al., 2003b). The PCA is applied to detect the concealed structure and associations of elements in the data set, in an attempt to explain the influence of latent factors on the data distribution (Simeonov *et al*., 2000; Krishna *et al*., 2011). Factor analysis had been used to identify the parameters that control trace metal distributions in the Mejillones Bay surface sediments (Loring, 1991; Selvaraj et al., 2004).

Table 5 shows Varimax rotated factor matrix results. Five components explained 95.85 % of the total variance in the 10 shale samples analysed. Component 1 accounts for 47.38 % of the total variance and group rare elements, MnO and all the trace elements except Co, P and U. This possibly indicates organic flux through the hydraulic transport is an efficient mechanism for non- detrital metal in the studied shale samples. The second component represents 22.37 % of the total variance and comprises of Co and all the major elements except SiO_2, CaO and Fe_2O_3. The strong association of these major elements indicates some degree of continental influence, especially kaolinite and halloysite minerals which were present at the bottom of shale sequence (Figure 3). The third component accounts for 13.38 % of the total variance and show association of CaO, Fe_2O_3, Na_2O, SiO_2, P_2O_5, P and Pb. This suggests the calcification of the shale sequence within the column of the ocean leading to the formation of grossite. The fourth component represents 6.99 % of the total variance and consists of SiO_2, Ni, Sr and P indicating the presence of detrital minerals such as quartz in the shale samples.

The fifth component represents 1.89 % of the total variance and comprises of Fe_2O_3, Na_2O, CaO and U. This indicates the presence of hematite minerals at the bottom of the shale sequence as revealed by XRD spectra results (Figure 4). This agrees with enrichment factor and paleo-redox indicators results that suggest oxidizing

environment of deposition.

5. Summary and conclusions

Based on the analysis of mineralogy and geochemical paleo-redox indicators for the Maastrichtian shales of Mamu Formation, southern Nigeria, the following conclusions may be drawn:

1. The basal part of the shale outcrop is characterized by quartz and kaolinite as the major crystalline minerals with traces of hematite. Similarly, the upper part consists of quartz and kaolinite as major crystalline minerals but with minor quantity of halloysite and grossite. The presence of hematite in the basal part of the shale outcrop suggests oxidizing diagenetic environment of deposition.
2. The ternary plot of the major elements shows that the shales are variably enriched with SiO_2 relative to Al_2O_3 and CaO. The positive correlations of K_2O, TiO_2, and Na_2O, with Al_2O_3 suggest that these elements are associated entirely with detrital phases.
3. The K_2O/Al_2O_3 ratio is close to the lower limit of clay mineral range, which suggests that kaolinite is the dominant clay minerals. The geochemical parameters such as Al_2O_3/TiO_2, low Cr/Ni, Th/Cr, Cr/Th, Th/Co and Th/Cr ratios suggest that felsic components dominated basement complex source rocks.
4. The CIA values indicate that these shales have experienced strong chemical weathering at the source area. In addition, the depletion of Na and Ca also illustrates an intense chemical weathering of the source rocks. The MIA values of the studied shale samples indicate an intense to extreme weathering of the mineralogical components.
5. The studied shales exhibit different degrees of trace-element enrichment, with the approximate order of enrichment relative to average shale being in the order: Co > Pb > Ni > Zr > Cu > Rb > V > Cr > Ba > V > Sr > U. The inverse correlation between changes in the oxidation state of the environment (Eh), pH, EC and TDS in studied shales may indicate oxygenated environment of deposition. Furthermore, the trace element redox indices ratios such as V/Cr, Ni/Co, Cu/Zn and U/Th infer that these shales were deposited under oxidizing diagenetic environment.

Acknowledgements

The authors sincerely acknowledge the technical assistance of the final year students who participated in the fieldwork (Sedimentary/Petroleum geology option 2011/2012 session). We wish to express our gratitude to Dr Remy Bucher, iTHEMBA labs, South Africa for XRD analysis, Ms. Melissa Crowley, XRF laboratory in the University of the Western Cape, South Africa for XRF analysis, and Ms. Riana Rossouw, LA-ICP-MS laboratory in the University of Stellenbosch for multi-element analysis.

References

Adebayo, O. F., Ojo, A. O. (2004). Palynostratigraphic of Cretaceous deposits of Anambra Basin, Eastern Nigeria. *Pakistan Journal of Scientific and Industrial Research*, 47(6), p. 417-422.

Agagu, O. K., Adighije, C. I. (1983). Tectonic and sedimentation framework of the lower Benue Trough, Southern Nigeria. *Journal of African Earth Science*, 1, p. 267-274.

Akaegbobi, M. I., Schmitt, M. (1998). "Organic Facies, Hydrocarbon Source Potential and the Reconstruction of the Depositional Paleoenvironment of the Campano-Maastrichtian Nkporo Shale in the Cretaceous Anambra Basin, Nigeria". *Nigerian Association of Petroleum Explorationists*, 13, p. 1-19.

Algeo, T. J., Maynard, J. B. (2004). Trace-element behavior and redox facies in core shales of Upper Pennsylvanian Kansas-type cyclothems. *Chemical Geology*, 206, p. 289– 318.

Armstrong-Altrin, J. S., Lee, Y. I., Verma, S. P., Ramasamy, S. (2004). Geochemistry of sandstones from the upper Miocene Kudankulam Formation, southern India: Implications for provenance, weathering, and tectonic setting. *Journal of Sedimentary Research*, 74(2), p.285-297.

Arnaboldi, M., Meyers, P. A. (2003). Geochemical evidence for paleoclimatic variations during deposition of two Late Pliocene sapropels from the Vrica section, Calabria. *Palaeogeography, Palaeoclimatology, Palaeoecology*, 190, p. 257- 271.

Berner, E. K., Berner, R. A. (1996). Global environment: water, air and geochemical cycles: Prentice Hall. New Jersey, 376 p.

Berner, R. A. (1971). Principles of chemical Sedimentology: McGraw Hill, Inc. USA.

Bjorlykke, K. (1974). Geochemical and mineralogical influence of Ordovician island arcs on epicontinental clastic sedimentation: a study of Lower Palaeozoic sedimentation in the Oslo region, Norway. *Sedimentology*, 21(2), p. 251-272.

Bock, B., McLennan, S.M., Hanson, G. N. (1998). Geochemistry and provenance of the Middle Ordovician Austin Glen Member (Normanskill Formation) and the Taconian Orogeny in New England. J. Sediment., 45, 635–655.

Braide, S. P. (1992). Syntectonic fluvial sedimentation in the central Bida Basin. *J. Mining and Geology*, 28, p. 55–64.
Brumsack, H. J. (1986). The inorganic geochemistry of Cretaceous black shales (DSDP Leg 41) in comparison to modern upwelling sediments from the Gulf of California: In Summerhayes, C.P., Shackleton, N.J. (Eds.), North Atlantic Palaeoceanography. *Spec. Publ.-Geol. Soc. Lond.,* vol. 21, p. 447– 462.
Brumsack, H. J. (1989). Geochemistry of recent TOC-rich sediments from the Gulf of California and the Black Sea. *Geologische Rundschau*, 78, p. 851–882.
Brumsack, H. J. (1980). Geochemistry of Cretaceous black shales from the Atlantic Ocean (DSDP Legs 11, 14, 36 and 41). *Chemical Geology*, 31, p. 1–25.
Calvert, S. E., Pedersen, T. F. (1993). Geochemistry of Recent oxic and anoxic marine sediments: implications for the geological record. *Marine Geology*, 113, p. 67– 88.
Chiaghanam O.I., Ikegwuonu, O.N., Chiadikobi, K.C., Nwozor K.K., Ofoma A.E., and Omoboriowo, A.O. (2012). Sequence Stratigraphy and Palynological Analysis of late Campanian to Maastrichtian Sediments in the Upper-Cretaceous, Anambra Basin. A Case Study of Okigwe and its Environs, South-Eastern, Nigeria. *Advances in Applied Science Research*, 3 (2), p. 962-979.
Condie, K.C., Boryta, M.D., Liu, J., Quian, X. (1992). The origin of khondalites: geochemical evidence from the Archean to Early Proterozoic granulitic belt in the North China Craton. *Precambrian Research*, 59(3-4), p. 207-223.
Cox, R., Lowe, D. R., Cullers, R. L. (1995). The influence of sediment recycling and basement composition on evolution of mudrock chemistry in the southwestern United States. *Geochimica et Cosmochimica Acta*, 59(14), p. 2919-2940.
Crusius, J., Calvert, S., Pedersen, T., Sage, D. (1996). Rhenium and molybdenum enrichments in sediments as indicators of oxic, suboxic and sulfidic conditions of deposition. *Earth Planet. Sci. Lett*. 145, p. 65–78.
Cullers, R. L. (1994). The controls on the major and trace element variation of shales, siltstones and sandstones of Pennsylvanian – Permian age from uplifted continental blocks in Colorado to platform sediment in Kansas, USA. *Geochimica et Cosmochimica Acta*, 58(22), p. 4955-4972.
Cullers, R. L. (1995). The controls on the major and trace element evolution of shales, siltstones and sandstones of Ordovician to Tertiary age in the Wet Mountain region, Colorado, U.S.A. *Chemical Geology*, 123(1-4), p. 107-131.
Cullers, R. L. (2000). The geochemistry of shales, siltstones and sandstones of Pennsylvanian-Permian age, Colorado, U.S.A. implications for provenance and metamorphic studies. *Lithos*, 51, p. 305-327.
Dean, W.E., Gardner, J.V., Piper, D. Z. (1997). Inorganic geochemical indicators of glacial – interglacial changes in productivity and anoxia of the California continental margin. *Geochim. Cosmochim. Acta*, 61, p. 4507– 4518.
Dean, W.E., Piper, D.Z., Peterson, L.C. (1999). Molybdenum accumulation in Cariaco basin sediment over the past 24 k.y.: a record of water-column anoxia and climate. *Geology*, 27, p. 507– 510.
Dill, H. (1986). Metallogenesis of early Paleozoic graptolite shales from the Graefenthal Horst (northern Bavaria-Federal Republic of Germany). *Economic Geology*, 81, p. 889-903.
Dill, H., Teshner, M., Wehner, H. (1988). Petrography, inorganic and organic geochemistry of Lower Permian Carboniferous fan sequences (Brandschiefer Series) FRG: constraints to their palaeogeography and assessment of their source rock potential. *Chemical Geology*, 67(3-4), p. 307-325.
Dypvik, H. (1984). Geochemical compositions and depositional conditions of Upper Jurassic and Lower Cretaceous Yorkshire clays, England. *Geological Magazine*, 121(5), p. 489-504.
Fedo, C. M., Eriksson, K., Krogstad, E. J. (1996). Geochemistry of shale from the Archean (~ 3.0 Ga) Buhwa Greenstone belt, Zimbabwe: Implications for provenance and source area weathering. *Geochimica et Cosmochimica Acta*, 60(10), p. 1751-1763.
Fedo, C. M., Nesbitt, H. W., and Young, G. M. (1995). Unravelling the effects of potassium metasomatism in sedimentary rocks and paleosols, with implications for paleoweathering condition and provenance. *Geology*, 23, 921-924.
Felix, N. S. (1977). Physico-chemical studies on bentonites with special reference to Fayoum Deposits: Ph.D. Thesis, Fac. of Sci., Cairo, Univ. Egypt.
Garrels, R. M., Mackenzie, F. T. (1971). Evolution of Sedimentary Rocks: Norton, New York, 397 pp.
Gill, S., and Yemane, K. (1996). Implications of a Lower Pennsylvanian Ultisol for equatorial Pangean climates and early, oligotrophic, forest ecosystems. *Geology,* Vol. 24., No. 10, p. 905-908.
Hallberg, R.O. (1976). A geochemical method for investigation of palaeoredox conditions in sediments: Ambio. *Special Report*, 4, p. 139-147.
Hatch, J. R., and Leventhal, J. S. (1992). Relationship between inferred redox potential of the depositional environment and geochemistry of the Upper Pennsylvanian (Missourian) Stark Shale Member of the Dennis

Limestone, Wabaunsee County, Kansas, U.S.A. *Chemical Geology*, 99, p. 65–82.
Hayashi, K., Fujisawa, H., Holland, H., Ohmoto, H. (1997). Geochemistry of ~1.9 Ga sedimentary rocks from northeastern Labrador, Canada. *Geochimica et Cosmochimica Acta*, 61(19), p. 4115-4137.
Helena B. A., Vega M., Barrado E., Pardo R., and Fernandez L. (1999). A case of hydrochemical characterization of an alluvial aquifer influenced by human activities. *Water Air Soil Pollut*., 112, p. 365–387.
Jones, B., Manning, D.A.C. (1994). Comparison of geological indices used for the interpretation of palaeoredox conditions in ancient mudstones. *Chemical Geology*, 111, p. 111-129.
Kassim, S. A. (2006). Paleoenvironmental Indicators of Clay Minerals in Miocene Sediments, Northern Iraq. *Damascus University Journal for Basic Sciences*, Vol. 22, No 1.
Krishna, K. A., Raman-Mohan, K., Murthy, N. N. (2011). A multivariate statistical approach for monitoring of heavy metals in sediments: a case study from Wailpalli Watershed, Nalgonda District, Andhra Pradesh, India. *Research Journal of Environmental and Earth Sciences*, 3(2), p. 103-113.
Liu, C. W., Lin, K. H., and Kuo, Y. M. (2003a). Application of factor analysis in the assessment of ground water quality in the Blackfoot disease area in Taiwan. *Sci. Total Environ*., 313, p.77–89.
Liu, W. X,, Li, X. D., Shen, Z. G., Wang, D. C., Wai, O. W. H., & Li, Y. S. (2003b). Multivariate statistical study of heavy metal enrichment in sediments of the Pearl River Estuary. *Environmental Pollution*, 121, p. 377-388.
Loring, D. (1991). Normalization of heavy metal data from estuarine and coastal sediments. ICES. *Journal of Marine Science*, 48, 101–115.
Madhavaraju, J., Ramasamy, S. (2002). Petrography and geochemistry of Late Maastrichtian - Early Paleocene sediments of Tiruchirapalli Cretaceous, Tamil Nadu - Paleoweathering and provenance implications. *Journal of the Geological Society of India*, 59, p. 133-142.
,Massart, D. L., Vandeginste B. G. M., Deming S. N., Michotte Y., Kaufman L. (1988). Chemometrics, A Textbook, Amsterdam: Elsevier.
Morford, J. L., Russell, A.D., Emerson, S. (2001). Trace metal evidence for changes in the redox environment associated with the transition from terrigenous clay to diatomaceous sediment, Saanlich Inlet, BC. *Marine Geology*, 174, p. 355– 369.
Nagarajan, R., Madhavaraju, J., Nagendra1, R., Armstrong-Altrin, J. S., and Moutte, J. (2007). Geochemistry of Neoproterozoic shales of the Rabanpalli Formation, Bhima Basin, Northern Karnataka, southern India: implications for provenance and paleoredox conditions. *Revista Mexicana de Ciencias Geológicas*, v. 24, núm. 2, p.150-160.
Nath, B.N., Bau, M., Ramalingeswara Rao, B., Rao, Ch. M. (1997). Trace and rare earth elemental variation in Arabian Sea sediments through a transect across the oxygen minimum zone. *Geochimica et Cosmochimica Acta*, 61(12), p. 2375-2388.
Nesbitt, H.W., Young, G. M. (1982). Early Proterozoic climates and plate motions inferred from major element chemistry of lutites. *Nature*, V. 299, p.715-717.
Nesbitt, H.W., Markovics, G., Price, R.C. (1980). Chemical processes affecting alkalies and alkaline earths during continental weathering. *Geochim. Cosmochim. Acta*, 44, p.1695 –1766.
Obaje, N. G., Musa, M. K., Odoma, A. N., and Hamza, H. (2011). The Bida Basin in north-central Nigeria: Sedimentology and petroleum geology: *Journal of Petroleum and Gas Exploration Research*, Vol. 1(1), pp. 001-013.
Ojo, O. J., Kolawole, A. U., and Akande, S. O. (2009). Depositional Environments, Organic Richness, and Petroleum Generating Potential of the Campanian to Maastrichtian Enugu Formation, Anambra Basin, Nigeria. *The Pacific Journal of Science and Technology*, 10, p. 614-627.
Pailler, D., Bard, E., Rostek, F., Zheng, Y., Mortlock, R., van Geen, A. (2002). Burial of redox-sensitive metals and organic matter in the equatorial Indian Ocean linked to precession: *Geochim. Cosmochim. Acta,* 66, p. 849–865.
Parham, W. E. (1966). Lateral variations in clay mineral assemblages in modern and ancient sediments: In proc. Int. Clay Conf. Jerusalem, 1, p. 136 – 145 (K. Gekker and A. Weiss, editors).
Piper, D. Z. (1994). Seawater as the source of minor elements in black shales, phosphorites, and other sedimentary deposits. *Chem. Geol*., 114, p. 95– 114.
Rimmer, S. M., (2004). Geochemical paleoredox indicators in Devonian–Mississippian black shales, Central Appalachian Basin (USA). *Chemical Geology*, 206, p. 373– 391.
Robert, C., and Kennett, J. P. (1994). Antarctic subtropical humid episode at the Paleocene-Eocene boundary: Clay mineral evidence. *Geology*, V.22, p. 211-214.
Ross, D. J. K., Bustin, and R. M. (2009). Investigating the use of sedimentary geochemical proxies for paleoenvironment interpretation of thermally mature organic-rich strata: Examples from the Devonian–Mississippian shales, Western Canadian Sedimentary Basin. *Chemical Geology*, 260, p. 1–19.

Selvaraj, K., Ram Mohan, V., Szefer, P. (2004). Evaluation of metal contamination in coastal sediments of the Bay of Bengal, India. geochemical and statistical approaches: *Marine Pollution Bulletin*, 49 (3), p. 174–185.
Shaw, T. J., Geiskes, J. M., Jahnke, R. A. (1990). Early diagénesis in differing depositional environments: the response of transition metals in pore water: *Geochimica et Cosmochimica Acta*, 54(5), p. 1233-1246.
Short, K. C., Stauble, A. J. (1967). Outline of Geology of Niger Delta. *American Association of Petroleum Geologists Bulletin*, 51, p. 761-779.
Simeonov, V., Massart, G., Andrew, G., and Tsakovski, S. (2000). Assessment of metal pollution based on multivariate statistical modelling of ''hot spot'' sediments from the Black sea. *Chemosphere*, 41, p. 1411-1417.
Unomah, G.I., and Ekweozor, C. M. (1993). "Petroleum Source Rock Assessment of the Campanian Nkporo Shale, Lower Benue Trough Nigeria". *Nigerian Association of Petroleum Explorationists Bulletin*, 8, p. 172-186.
Voicu, G., and Bardoux, M. (2002). Geochemical behaviour under tropical weathering of the Barama-Mazaruni greenstone belt at Omai gold mine, Guiana Shield. *Applied Geochemistry*, 17, p. 321-336.
Voicu, G., Bardoux, M., Harnois, L., and Grepeau, R. (1997). Lithological and geochemical environment of igneous and sedimentary rocks at Omai gold mine, Guyana, South America. *Exploration and Mining Geology*, 6, p. 153-170.
Warning, B., Brumsack, H. J. (2000). Trace metal signatures of eastern Mediterranean sapropels. *Palaeogeography, Palaeoclimatology, Palaeoecology*, 158, p. 293–309.
Weaver, C. E. (1960). Possible uses of clay minerals in search for oil. *American association of Petroleum Geologists Bulletin*, 44, p. 1505-1518.
Wedepohl, K.H. (1971). Environmental influences on the chemical composition of shales and clays. In: Ahrens, L.H., Press, F., Runcorn, S.K., Urey, H.C. (Eds.). *Physics and Chemistry of the Earth*, vol. 8. Pergamon, Oxford, p. 307–331.
Willet, P. (1987). Similarity and Clustering in Chemical Information Systems. Chichester: Wiley. Research Studies Press.
Wronkiewicz, D. J., Condie, K. C. (1990). Geochemistry and mineralogy of sediments from the Ventersdorp and Transvaal Supergroups, South Africa: Cratonic evolution during the early Proterozoic. *Geochimica et Cosmochimica Acta*, 54(2), p. 343-354.
Yarincik, K.M., Murray, R.W., Lyons, T.W., Peterson, L.C., Haug, G.H. (2000). Oxygenation history of bottom waters in the Cariaco Basin, Venezuela, over the past 578,000 years: results from redox-sensitive metals (Mo, V, Mn, and Fe). *Paleoceanography*, 15, p. 593– 604.

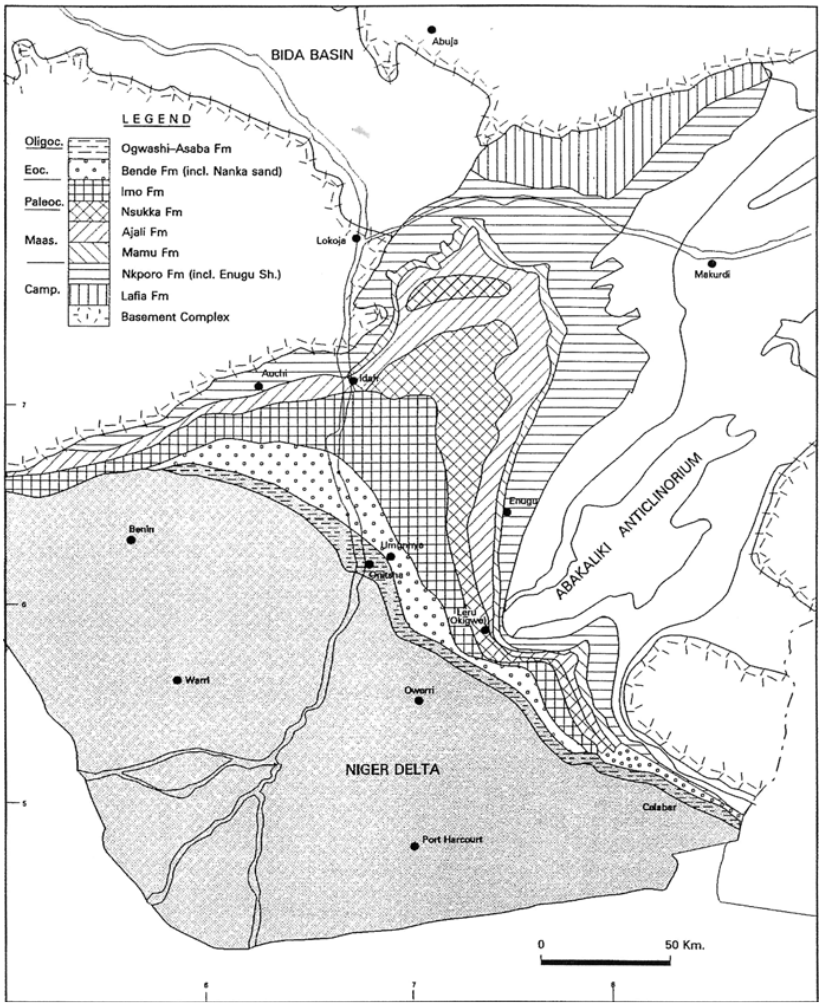

Figure 1. Geological sketch map of the Anambra Basin, Nigeria.

Figure 2. Maastrichtian shale facies of Mamu Formation exposed at Auchi-Igarra Road.

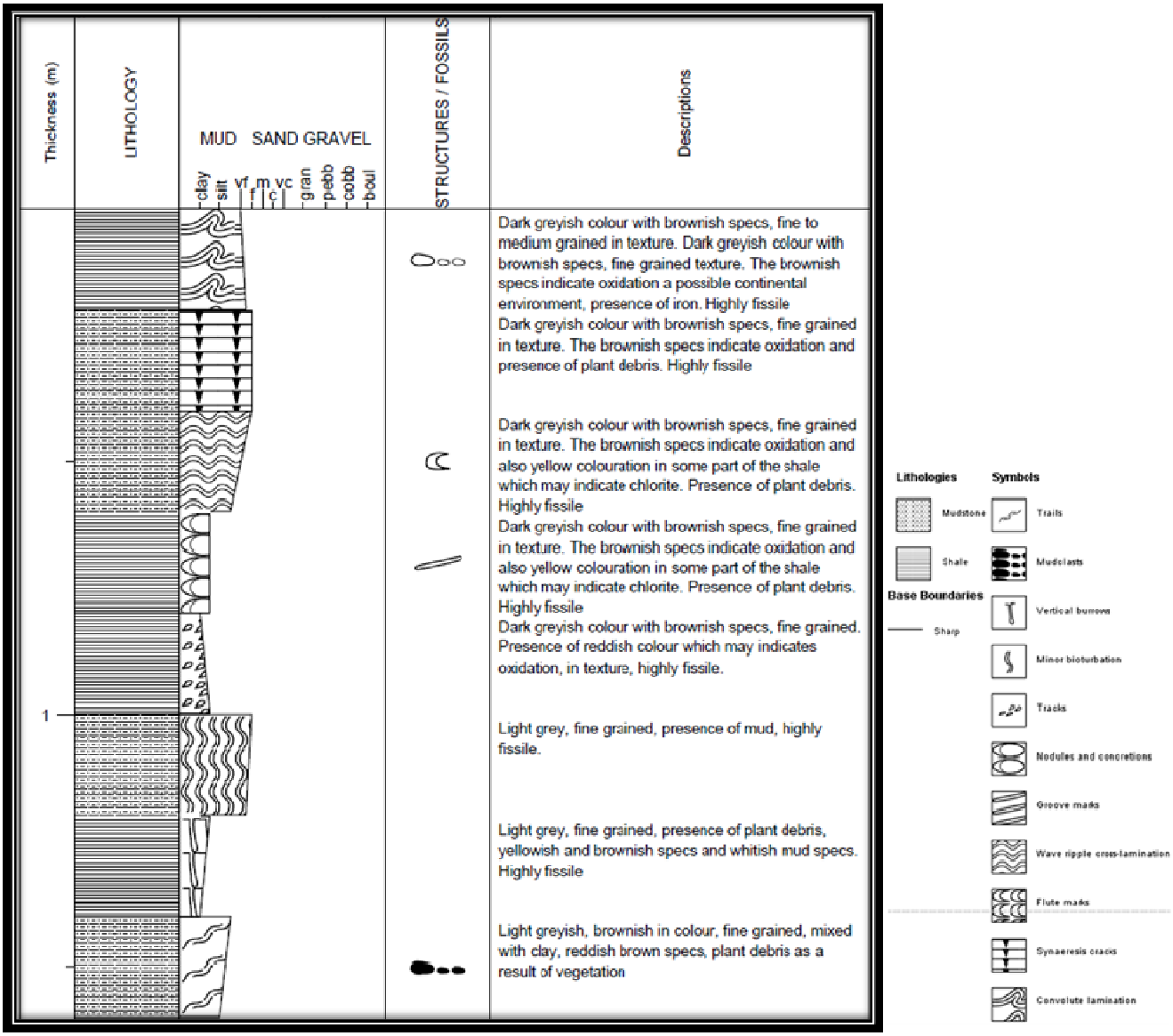

Figure 3. Lithologic section of Maastrichtian shale outcrop at Auchi-Igarra Road, Nigeria.

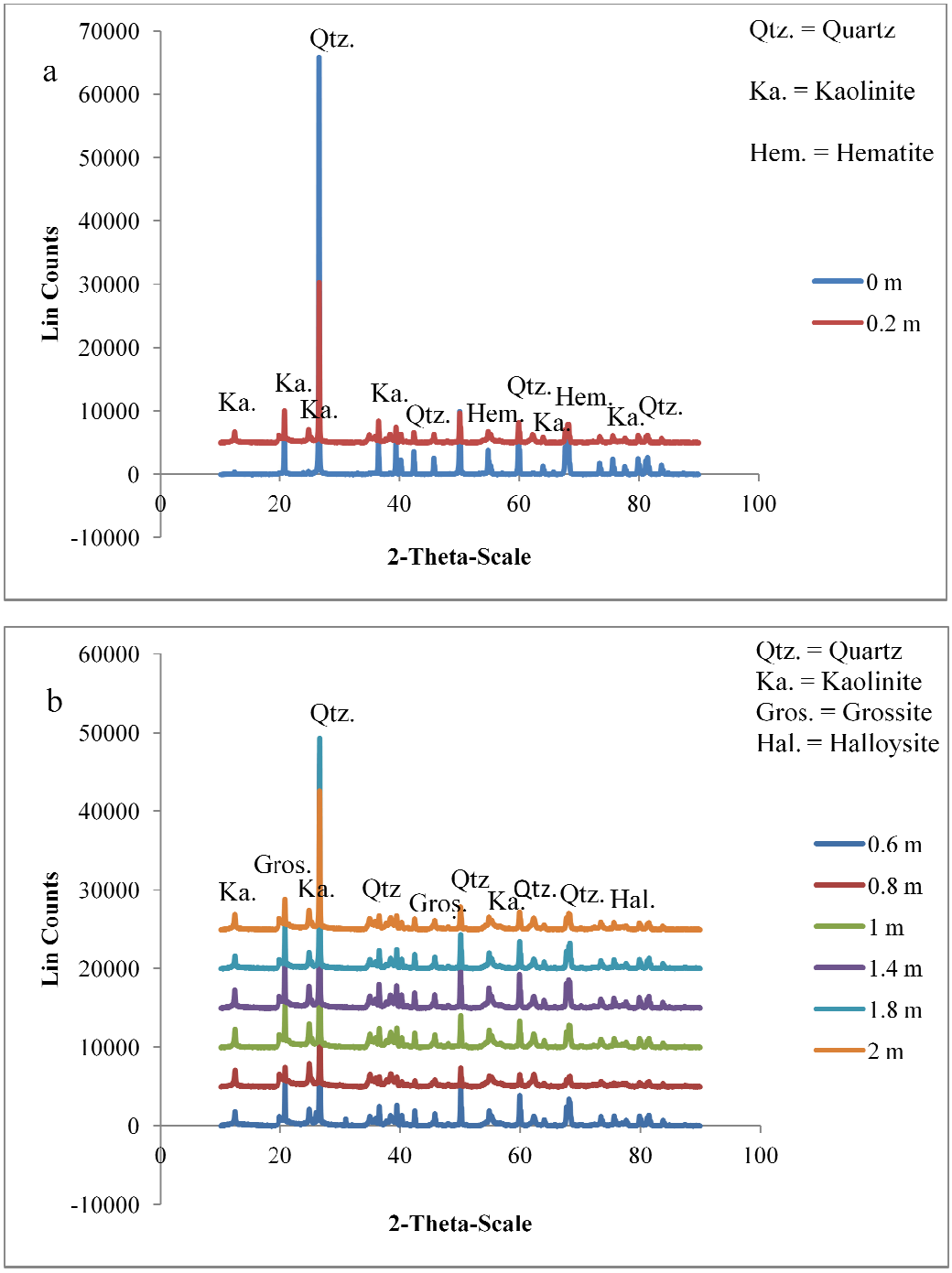

Figure 4. Characteristic X-ray diffraction spectra of shale samples from (a) first geochemically specific interval (i.e. 0.0 -0.2 m) and (b) second geochemically specific interval (i.e. 0.6 – 2m).

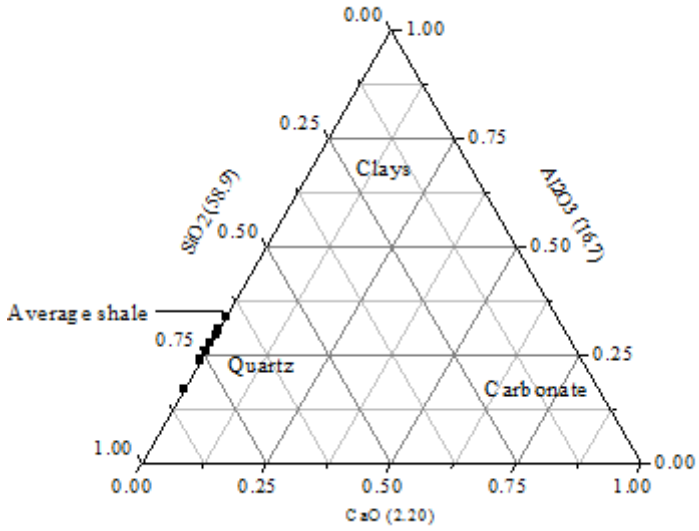

Figure 5. Ternary diagram showing relative proportions of shale/mudrock major elements SiO_2 (quartz), Al_2O_3 (clays) and CaO (carbonates). Average shale also shown as checked box (after Wedepohl, 1971).

Table 1. Correlation Chart for Early Cretaceous-Tertiary strata in southeastern Nigeria (modified from Nwajide, 1990).

	AGE	ABAKALIKI – ANAMBRA BASIN	AFIKPO BASIN
m.y 30	Oligocene	Ogwashi-Asaba Formation	Ogwashi-Asaba Formation
54.9	Eocene	Ameki/Nanka Formation/ Nsugbe Sandstone (Ameki Group)	Ameki Formation
65	Palaeocene	Imo Formation	Imo Formation
		Nsukka Formation	Nsukka Formation
	Maastrichtian	Ajali Formation	Ajali Formation
73		Mamu Formation	Mamu Formation
	Campanian	Nkporo Shale /Oweli Formation/Enugu Shale (Nkporo Group)	Nkporo Shale/ Afikpo Sandstone
83	Santonian		Non-deposition/erosion
87.5	Coniacian	Agbani Sandstone/Awgu Shale	
88.5	Turonian	Eze Aku Group	Eze Aku Group (incl. Amasiri Sandstone)
93	Cenomanian – Albian	Asu River Group	Asu River Group
100			
119	Aptian Barremian Hauterivian	Unnamed Units	
Precambrian		Basement Complex	

Table 2. Pearson's coefficient correlations for all geochemical parameters measured in extracted interstitial pore water of the Cretaceous shales

	pH	Ec	TDS	Eh	Ca	Mg	Na	K	F	Cl
pH	1									
Ec	**0.85**	1								
TDS	**0.85**	**0.99**	1							
Eh	-0.83	-0.86	-0.861	1						
Ca	**0.93**	**0.96**	**0.96**	-0.84	1					
Mg	**0.94**	**0.95**	**0.95**	-0.81	**0.99**	1				
Na	**0.41**	**0.29**	**0.29**	-0.21	**0.37**	**0.45**	1			
K	**0.75**	**0.77**	**0.77**	-0.61	**0.80**	**0.86**	**0.81**	1		
F	**0.85**	**0.90**	**0.90**	-0.84	**0.93**	**0.93**	**0.57**	**0.88**	1	
Cl	0.07	0.04	0.04	0.00	0.08	0.15	**0.92**	**0.60**	**0.34**	1

Significant values ($p < 0.05$) are shown in bold.

Table 3. Major elements (wt %), trace elements (mg/kg) and element ratios in the studied shales

Major elements (wt %)											
Sample name	Average shale	C 0.0m	C 0.2m	C 0.4m	C 0.6m	C 0.8m	C 1.0m	C 1.4m	C 1.6m	C 1.8m	C 2.0m
Al_2O_3	16.7	3.42	19.56	21.49	14.82	26.46	23.25	24.86	20.01	*nd*	24.22
CaO	2.20	0.08	0.02	0.02	0.04	0.06	0.02	0.04	0.04	*nd*	0.07
Cr_2O_3	*nd*	0.00	0.02	0.02	0.01	0.03	0.02	0.02	0.02	*nd*	0.02
Fe_2O_3	6.90	3.15	3.56	1.55	2.75	2.26	1.62	1.94	1.46	*nd*	1.67
K_2O	3.60	0.15	1.00	1.07	0.74	1.41	1.00	1.20	0.97	*nd*	1.20
MgO	2.60	0.10	0.25	0.27	0.20	0.35	0.22	0.29	0.22	*nd*	0.30
MnO	*nd*	0.00	0.01	0.01	0.01	0.01	0.01	0.01	0.00	*nd*	0.00
Na_2O	1.60	0.08	0.10	0.06	0.08	0.07	0.06	0.06	0.05	*nd*	0.05
P_2O_5	*nd*	0.10	0.11	0.09	0.10	0.17	0.07	0.12	0.08	*nd*	0.07
SiO_2	58.9	92.20	63.62	62.48	72.77	51.83	61.22	56.52	64.49	*nd*	58.27
TiO_2	0.78	0.29	1.42	1.57	1.09	1.10	1.55	1.33	1.61	*nd*	1.41
LOI	*nd*	1.81	10.79	11.15	7.92	16.16	11.52	13.84	10.45	*nd*	12.70
Sum Of Conc.	*nd*	101.37	100.45	99.77	100.53	99.90	100.56	100.23	99.39	*nd*	99.97
Trace elements (mg/kg)											
Sample name	Average shale	C 0.0m	C 0.2m	C 0.4m	C 0.6m	C 0.8m	C 1.0m	C 1.4m	C 1.6m	C 1.8m	C 2.0m
Ni	68	0.00	8	6	5	49	9	28	*nd*	34	7
Cu	45	1	8	18	13	14	12	9	*nd*	12	12
Zn	95	19	35	29	26	35	29	23	*nd*	25	26
Ga	*nd*	4	25	28	24	34	28	26	*nd*	24	32
Rb	140	6	55	59	46	79	54	53	*nd*	54	66
Sr	300	24	100	106	87	155	92	100	*nd*	101	96
Y	*nd*	8	50	56	48	56	51	53	*nd*	55	53
Zr	160	117	355	424	401	234	350	397	*nd*	380	302
Nb	*nd*	7	28	30	30	24	31	30	*nd*	32	28
Pb	22	136	151	154	149	163	152	152	*nd*	152	149
Th	*nd*	1.00	16	20	16	13	17	20	*nd*	19	14
U	3.7	*nd*	2.00	*nd*	*nd*	*nd*	*nd*	*nd*	*nd*	0.00	0.00
Ti	*nd*	1991	10495	10970	10812	8089	10844	10787	*nd*	11278	10009
V	130	42	235	248	239	185	247	242	*nd*	253	223
Cr	90	28	144	162	135	184	168	127	*nd*	140	161
Co	19	159	51	36	47	47	25	45	*nd*	39	40
Ba	580	34	233	274	247	346	272	267	*nd*	271	268
La	*nd*	13	63	71	71	89	78	93	*nd*	92	78
Ce	*nd*	11	203	212	133	210	190	245	*nd*	215	228
Nd	*nd*	15	73	84	60	97	75	100	*nd*	99	97
P	*nd*	639	520	480	311	720	311	382	*nd*	403	288
Major and trace elements ratios											
Sample name	C 0.0m	C 0.2m	C 0.4m	C 0.6m	C 0.8m	C 1.0m	C 1.4m	C 1.6m	C 1.8m	C 2.0m	
CIA	91.75	94.60	94.95	94.54	94.53	95.57	95.01	95.01	*nd*	95.10	
MIA	83.49	89.20	89.89	89.08	89.06	91.14	90.03	90.01	*nd*	90.21	
SiO_2/Al_2O_3	26.95	3.25	2.91	4.91	1.96	2.63	2.27	3.22	*nd*	2.41	
Na_2O/K_2O	0.51	0.10	0.06	0.11	0.05	0.06	0.05	0.05	*nd*	0.04	
K_2O/Al_2O_3	0.04	0.05	0.05	0.05	0.05	0.04	0.05	0.05	*nd*	0.05	
Al_2O_3/TiO_2	11.96	13.74	13.71	13.57	24.06	14.96	18.73	12.46	*nd*	17.19	
Ni/Co	*n.d*	0.36	0.16	0.17	0.11	1.04	0.62	*nd*	0.87	0.18	
V/Cr	1.50	1.47	1.63	1.53	1.77	1.01	1.91	*nd*	1.81	1.39	
U/Th	*nd*	*nd*	0.13	*nd*	*nd*	*nd*	*nd*	*nd*	*nd*	*nd*	
Cr/Ni	nd	18	27	27	3.76	18.67	4.54	*nd*	4.12	23.00	
Cr/Th	28	9	8.1	8.44	14.15	9.88	6.35	*nd*	7.37	11.50	
Th/Co	0.006	0.31	0.56	0.34	0.28	0.68	0.44	*nd*	0.49	0.35	
Th/Cr	0.036	0.11	0.12	0.12	0.07	0.10	0.16	*nd*	0.14	0.09	
Cu/Zn	0.053	0.23	*0.62*	0.50	0.4	0.41	0.39	*nd*	0.48	0.46	

Average shale data from Wedepohl (1971, 1991); Brumsack, 2006.

Table 4. Enrichment factors for some selected trace elements in the studied shale samples

Element	Average shale	C 0.0 m	C 0.2 m	C 0.4 m	C 0.6 m	C 0.8 m	C 1.0 m	C 1.4 m	C 1.6 m	C 1.8 m	C 2 m
Ni (ppm)	68	0.00	8	6	5	49	9	28	0.00	34	7
$(Ni/Al)*10^4$	7.7	0.00	0.77	0.53	0.64	3.50	0.73	2.13	0.00	0.00	0.55
EF		0.00	0.10	0.68	1.21	5.49	0.21	2.91	0.00	0.00	0.07
Co (ppm)	19	159	51	36	47	47	25	45	0.00	39	40
$(Co/Al)*10^4$	2.1	87.82	4.93	3.16	5.99	3.36	2.03	3.42	0.00	0.00	3.12
EF		41.82	0.06	0.64	1.89	0.56	0.61	1.68	0.00	0.00	1.49
Cu (ppm)	45	1	8	18	13	14	12	9	0.00	12	12
$(Cu/Al)*10^4$	5.1	0.55	0.77	1.58	1.66	1.00	0.98	0.68	0.00	0.00	0.94
EF		0.11	1.40	2.05	1.05	0.60	0.98	0.70	0.00	0.00	0.18
Zn (ppm)	95	19	35	29	26	35	29	23	0.00	25	26
$(Zn/Al)*10^4$	11	10.49	3.38	2.55	3.31	2.50	2.36	1.75	0.00	0.00	2.03
EF		0.95	0.32	0.75	1.30	0.75	0.94	0.74	0.00	0.00	0.18
V (ppm)	130	42	235	248	239	185	247	242	0.00	253	223
$(V/Al)*10^4$	15	23.20	22.70	21.80	30.46	13.21	20.07	18.39	0.00	0.00	17.39
EF		1.55	0.98	0.96	1.40	0.43	1.52	0.92	0.00	0.00	1.16
Cr (ppm)	90	28	144	162	135	184	168	127	0.00	140	161
$(Cr/Al)*10^4$	10.2	15.47	13.91	14.24	17.20	13.14	13.65	9.65	0.00	0.00	12.56
EF		1.52	0.90	1.02	1.21	0.76	1.04	0.71	0.00	0.00	1.23
Ba (ppm)	580	34	233	274	247	346	272	267	0.00	271	268
$(Ba/Al)*10^4$	66	18.78	22.50	24.08	31.48	24.70	22.10	20.29	0.00	0.00	20.90
EF		0.28	1.20	1.07	1.31	0.78	0.89	0.92	0.00	0.00	0.32
Rb (ppm)	140	6	55	59	46	79	54	53	0.00	54	66
$(Rb/Al)*10^4$	16	3.31	5.31	5.19	5.86	5.64	4.39	4.03	0.00	0.00	5.15
EF		0.21	1.60	0.98	1.13	0.96	0.78	0.92	0.00	0.00	0.32
Sr (ppm)	300	24	100	106	87	155	92	100	0.00	101	96
$(Sr/Al)*10^4$	34	13.26	9.66	9.32	11.09	11.07	7.48	7.60	0.00	0.00	7.49
EF		0.39	0.73	0.96	1.19	1.00	0.68	1.02	0.00	0.00	0.22
Zr (ppm)	160	117	355	424	401	234	350	397	0.00	380	302
$(Zr/Al)*10^4$	18	64.62	34.29	37.27	51.10	16.71	28.44	30.18	0.00	0.00	23.55
EF		3.59	0.53	1.09	1.37	0.33	1.70	1.06	0.00	0.00	1.31
Pb (ppm)	22	136	151	154	149	163	152	152	0.00	152	149
$(Pb/Al)*10^4$	2.5	75.12	14.58	13.54	18.99	11.64	12.35	11.55	0.00	0.00	11.62
EF		30.05	0.19	0.93	1.40	0.61	1.06	0.94	0.00	0.00	4.65
U (ppm)	3.7	0.00	2.00	0.00	0.00	0.00	0.00	0.00	0.00	0.00	0.00
$(U/Al)*10^4$	0.42	0.00	0.19	0.00	0.00	0.00	0.00	0.00	0.00	0.00	0.00
EF		0.00	0.46	0.00	0.00	0.00	0.00	0.00	0.00	0.00	0.00

[a] Calculated average shale data (Wedepohl , 1971, 1991; Rimmer, 2004; Brumsack, 2006. Nagarajan et al., 2007).
[b] Mean Al content for average shale: 8.84% (Wedepohl, 1971).

Table 5. Varimax Rotated Factor Loadings Matrix and Communalities Obtained from Principal Component Analysis for the Studied Major, Trace and Rare earth Elements in the shale samples

Variables	Comp. 1	Comp. 2	Comp. 3	Comp. 4	Comp.5	Communalities
MnO	0.54	0.52			0.43	0.79
K_2O		0.98				0.99
Cr_2O_3		0.98				0.99
Al_2O_3		0.98				0.99
LOI		0.97				0.99
MgO		0.95				0.99
TiO_2		0.89				0.98
P_2O_5		0.66	0.65			0.93
Fe_2O_3			0.83		0.40	0.96
Na_2O		0.41	0.73		0.44	0.99
SiO_2			0.70	-0.50		0.99
CaO			0.67		-0.55	0.90
Ni	0.41			0.88		0.95
Co		-0.53	0.80			0.96
V	0.98					0.99
Cr	0.94					0.96
Cu	0.90					0.86
Zn	0.85					0.95
Pb	0.88		0.42			0.99
Rb	0.89					0.97
Sr	0.86			0.42		0.99
Ba	0.93					0.99
Nb	0.98					0.99
P			0.72	0.49		0.93
Ti	0.97					0.99
Y	0.97					0.99
Th	0.94					0.96
Zr	0.94					0.96
U					0.89	0.84
La	0.93					0.97
Ga	0.92					0.98
Nd	0.91					0.96
Ce	0.91					0.94
EV	15.64	7.38	4.42	2.31	1.89	
VAR (%)	47.38	22.37	13.38	6.99	5.72	
CVAR (%)	47.38	69.75	83.13	90.13	95.85	